

**Invited paper**

## Luminescence and optical properties of siloxene

M. Stutzmann, M.S. Brandt, M. Rosenbauer, H.D. Fuchs, S. Finkbeiner, J. Weber and P. Deak

*Max-Planck-Institut für Festkörperforschung, Heisenbergstraße 1, 70569 Stuttgart, Germany*

We review the optical and luminescence properties of siloxene ( $\text{Si}_6\text{O}_3\text{H}_6$ ). The preparation and basic structural properties of siloxene are described, and theoretical results concerning optical transitions in different modifications of siloxene are discussed. The dominant structural building blocks in as-prepared siloxene are two-dimensional Si planes which give rise to a direct band gap in the visible energy range. The optical properties of annealed siloxene originate from isolated  $\text{Si}_6$  rings which act as radiative recombination centers. The luminescence of annealed siloxene and porous silicon are compared in detail. In particular, new experimental results based on optically detected magnetic resonance provide microscopic information about radiative states in porous Si which is incompatible with the conventional quantum confinement model.

### 1. Introduction

Siloxene ( $\text{Si}_6\text{O}_3\text{H}_6$ ) is one of the few silicon-based materials which show strong photoluminescence even at room temperature. Although already discovered as early as 1863 by Wöhler [1], up to now only a few groups have studied in detail different properties of siloxene or its derivatives [2–6]. Early investigations have mainly concentrated on the preparation and chemical aspects of siloxene, with only little quantitative information about optical properties [2,3]. A structural investigation of siloxene was performed by Weiss et al. in 1979 [4] using X-ray diffraction. Finally, in two short articles the group of Morigaki at the University of Tokyo has published more detailed results concerning the structure, absorption and luminescence of as-prepared and annealed siloxene [5,6].

Renewed interest in siloxene and related compounds was generated by our suggestion that this class of materials may also be responsible for the strong visible luminescence in porous silicon [7,8]. This proposal was based on a comparison of vibrational and luminescence spectra of porous silicon

and annealed siloxene. In the meantime, we have performed a much more detailed investigation of most aspects of optical processes in both porous Si and siloxene, which will be presented below. Our results provide further strong evidence for the hypothesis that radiative centers in annealed siloxene are identical to those in porous Si, despite recent criticism based mainly on indirect structural arguments [9,10].

### 2. Preparation and structural properties of siloxene

Following the recipe given by Wöhler, siloxene is prepared via a topochemical reaction starting from metallic  $\text{CaSi}_2$ .  $\text{CaSi}_2$  is obtained from a high temperature ( $T \geq 800^\circ\text{C}$ ) reaction between Si and Ca and consists of alternating layers of Ca (monolayers) and Si (double layers). Commercial (technical grade)  $\text{CaSi}_2$  contains a certain fraction of silicon crystallites and it has been argued that these crystallites are mainly responsible for the optical properties of siloxene prepared from  $\text{CaSi}_2$  [11]. However, it is also possible to grow epitaxial  $\text{CaSi}_2$  layers on Si (111) surfaces which do not contain any noticeable amount of Si crystallites [12], but after chemical transformation still show the same optical and luminescence properties as siloxene obtained

*Correspondence to:* Dr. M. Stutzmann, Max-Planck-Institut für Festkörperforschung, Heisenbergstraße 1, 70569 Stuttgart, Germany.

from commercial  $\text{CaSi}_2$ . Therefore, spurious contributions of Si microcrystals to the optical spectra of siloxene discussed below can be safely excluded.

For the preparation of siloxene, (poly) crystalline  $\text{CaSi}_2$  is exposed to aqueous HCl at  $0^\circ\text{C}$  for several hours in the absence of UV light and ambient gases. The ensuing reaction removes the calcium layers via formation of  $\text{CaCl}_2$ . The remaining double layers of Si are passivated by hydrogen and/or hydroxyl radicals as shown schematically in Fig. 1. Depending on the details of the reaction process, two forms of siloxene can be obtained [1,2]:

- Kautsky siloxene, which comes closest to the ideal structure shown below, but is very reactive in the presence of air, and
- Wöhler siloxene, which constitutes a less-ordered conformation of siloxene. Wöhler siloxene has approximately the same stoichiometry and bonding configurations as Kautsky siloxene, but is more inert to ambient gases due to a yet unknown surface passivation of the siloxene crystallites.

Because it is much easier to handle, most of the experimental results presented below pertain to Wöhler siloxene.

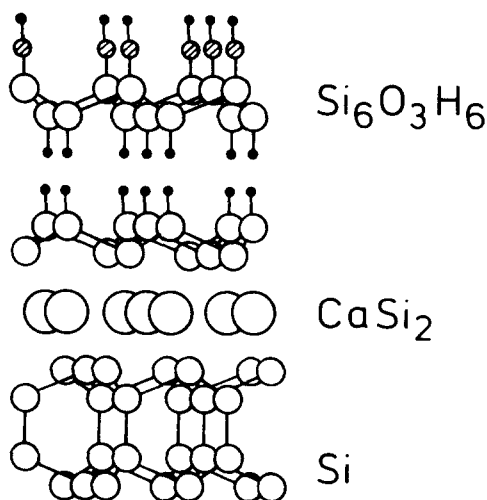


Fig. 1. Schematic view of the preparation of siloxene ( $\text{Si}_6\text{O}_3\text{H}_6$ ) from  $\text{CaSi}_2$ . Si and Ca atoms are indicated by small and large open circles, respectively, and O and H atoms by hatched circles and small full circles, respectively.

The idealized structure of stoichiometric crystalline siloxene is shown in Fig. 2 (left). The Si double layers present in the parent  $\text{CaSi}_2$  crystal remain essentially intact, with the intercalated Ca layers replaced by dissociated water molecules. One side of the Si double layer is passivated by hydrogen, whereas the opposite side is passivated by OH radicals. The overall stoichiometry is  $\text{Si}_6\text{O}_3\text{H}_6$ , as corroborated by a quantitative chemical analysis. Passivated double layers are stacked upon each other to form the three-dimensional siloxene crystal. X-ray diffraction studies performed on siloxene crystals [4] or powders [8] show that the Si–Si bonding distance within a double layer is essentially preserved, whereas the layer-to-layer spacing is about  $6.2 \text{ \AA}$ , much larger than in crystalline silicon. The presence of OH and H as bond terminators can be deduced unambiguously from the infrared absorption spectra of as-prepared siloxene [8,13]. In addition, X-ray absorption fine structure spectra as well as infrared absorption data indicate the presence of certain amounts of Si and  $\text{SiO}_2$  precipitates.

When as-prepared siloxene is heated in ambient atmosphere, the two-dimensional Si double layers are destroyed by insertion of oxygen atoms. This is an exothermic process occurring spontaneously upon thermal or optical excitation and resulting eventually in the idealized structure shown in Fig. 2 (right). There, sixfold silicon rings are connected via oxygen bridges, with the remaining silicon bonds terminated by hydrogen. Quantum chemical calculations indicate that this structure is the lowest energy configuration of stoichiometric siloxene. This structure can be obtained from that shown in Fig. 2 (left) by insertion of oxygen atoms from OH radicals into the Si double layers. Such a reaction occurs at temperatures above  $\approx 200^\circ\text{C}$  and can be followed by corresponding changes in the infrared absorption spectra [8]. Detailed studies of the structural and vibrational properties of annealed siloxene have shown that this material is best described as an amorphous, substoichiometric Si:O:H alloy [5,8,13]. Loss of long-range order occurs mainly by random oxygen insertion, hydrogen loss and cross-linking of adjacent Si planes by oxygen bridges caused by over-oxidation. In particular, the vibrational spectroscopy data suggest

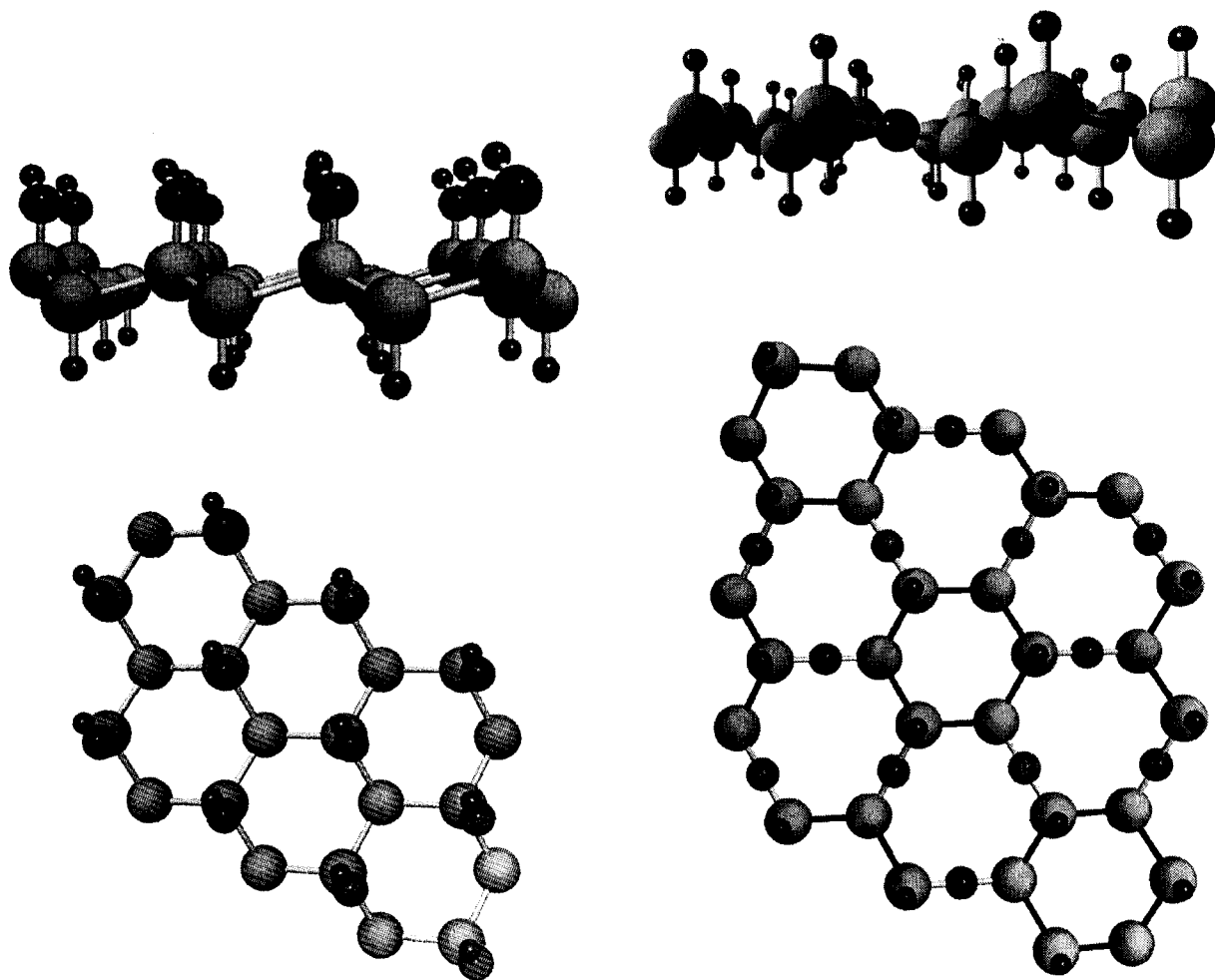


Fig. 2. Atomic structure of as-prepared (left side) and annealed siloxene (right side). Both side views and top views are shown.

that, for annealing temperatures below 400°C, annealed siloxene still maintains a considerable fraction of the Si backbone structure present in as-prepared samples (sixfold silicon rings).

### 3. Optical properties

Compared to crystalline Si with its indirect gap at 1.1 eV and the first direct gap at 3.4 eV, the optical properties of siloxene are quite different and depend strongly on the detailed bonding and oxidation state. Theoretical investigations indicate that as-prepared siloxene with a two-dimensional

arrangement of silicon atoms should have a direct band gap of the order of 1.5 to 2.7 eV, depending on the computational method employed [14,15]. The possibility of strong direct optical transitions in an ordered silicon-based material is a unique feature of as-prepared siloxene, and certainly deserves further attention in the future. Upon destruction of the Si planes by insertion of oxygen, the band structure changes again back to that of an indirect semiconductor. The structural unit important for the optical properties of annealed, oxidized siloxene are isolated  $\text{Si}_6$  rings separated from one another by bridging oxygen atoms (cf. Fig. 2 (right)). Optical excitation of such  $\text{Si}_6$  rings is expected to occur

most efficiently via the lowest direct transition in the vicinity of 4 eV. Further details of the band structure of stoichiometric siloxene ( $\text{Si}_6\text{O}_3\text{H}_6$ ) are shown in Fig. 3, both for the Si plane structure (cf. Fig. 2 (left)) and for the  $\text{Si}_6$ -ring conformation (Fig. 2 (right)). Since the latter siloxene structure will be of particular importance for the comparison with porous Si, we also show in Fig. 4 a schematic view of the electronic wave functions forming the

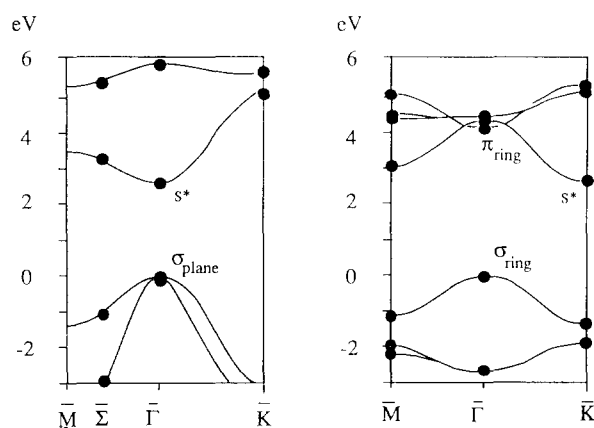


Fig. 3. Electronic band structure of the two-dimensional Si planes in as-prepared siloxene (left) and of a periodic array of isolated  $\text{Si}_6$ -rings in idealized annealed siloxene (right).

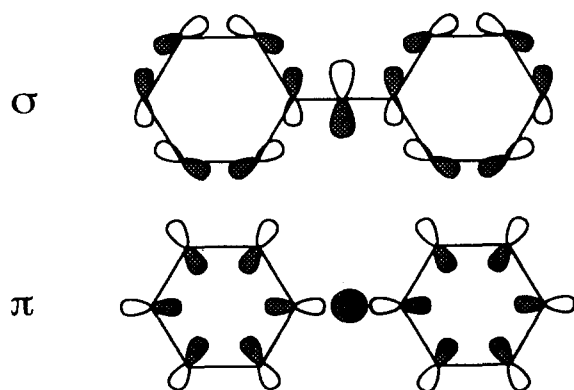


Fig. 4.  $\sigma$ - and  $\pi$ -bonded combinations of the Si 3p-orbitals forming the top of the valence band and the bottom of the conduction band of stoichiometric siloxene in the  $\text{Si}_6$ -ring configuration. Shown are two adjacent Si rings together with one bridging oxygen atom.

top of the valence band and the bottom of the conduction band at the center of the two-dimensional Brillouin zone. The top of the valence band is formed by  $\sigma$ -bonds between Si  $p_x$ - and  $p_y$ -orbitals, whereas the bottom of the conduction band is constructed out of  $\pi$ -bonds between the same atomic orbitals. Towards the edges of the Brillouin zone, these  $\pi$ -bonded orbitals of the  $\text{Si}_6$  rings are replaced by antibonding  $s^*$ -orbitals.

A particular feature of siloxene in the ring configuration is the sensitivity of the lowest optical transition energies to the nature of the ligands connected to the silicon atoms forming a  $\text{Si}_6$  ring. In stoichiometric siloxene, each silicon atom is bonded to one oxygen atom, two silicon atoms, and one hydrogen atom (see Fig. 2 (right)). The hydrogen atoms only serve as a bond termination with no structural importance. Therefore, each H atom can be replaced by other monovalent radicals, such as Cl,  $\text{NH}_2$ , OH, etc. Strongly electronegative ligands such as OH extract electronic density from the Si orbitals of the rings and thus reduce the bonding-antibonding splitting between the top of the valence band and the bottom of the conduction band. Indeed, it is found in computer simulations that further oxidation of  $\text{Si}_6$  rings by bond termination with OH groups or by cross-linking of adjacent rings via oxygen bridges will reduce the band gap of siloxene in six discrete steps from approximately 3 eV to about 1.5 eV [2,14].

In Fig. 5, we have summarized the experimentally observed fundamental optical properties of as-prepared siloxene at 300 K and at low temperatures. Most remarkable is the strong luminescence in the green to blue spectral range ( $\approx 2.4$  eV) in accordance with the theoretical prediction of a dipole-allowed direct gap for the two-dimensional Si planes. Excitation of the luminescence occurs most effectively in a narrow band centered around 2.5 eV (Fig. 5(b)). The spectral position of this band also coincides with the onset of absorption as shown in Fig. 4(c). At low temperatures, both the luminescence excitation and the optical absorption spectra shift to higher energies by about 0.1 eV. The coincidence of optical absorption, luminescence excitation and luminescence in a relatively narrow energy window between 2.3 and 2.6 eV suggests an excitonic nature of the lowest

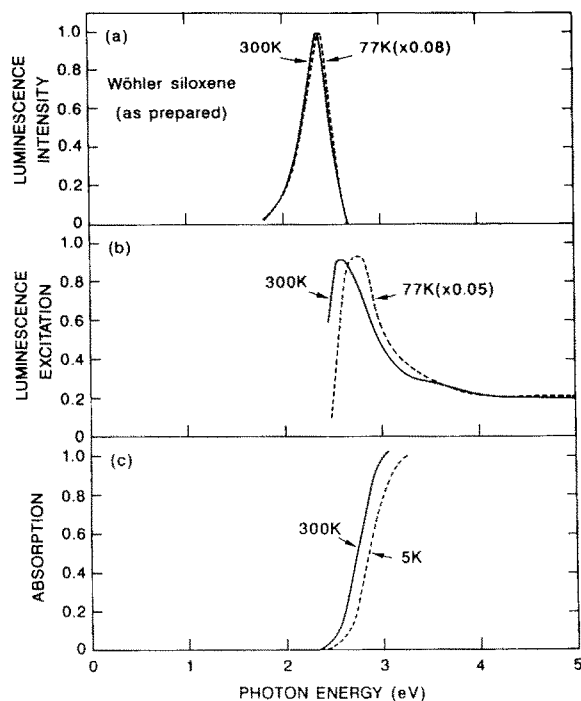


Fig. 5. Luminescence spectra (a), luminescence excitation spectra (b) and optical absorption spectra (c) of as-prepared Wöhler siloxene at 300 K (solid curves) and at low temperatures (dashed curves, 5 and 77 K) as a function of photon energy.

optical transitions. This conclusion is further corroborated by the observation of distinct triplet-exciton features in optically detected magnetic resonance (ODMR, see also below).

The pronounced changes in the optical properties of siloxene produced by thermal annealing are shown in Fig. 6. Whereas as-prepared siloxene, which consists mainly of Si planes, absorbs in the blue and luminesces in the green, the partially oxidized  $\text{Si}_6$  rings characteristic for annealed siloxene absorb and luminesce in the red. Note also that the luminescence excitation of annealed siloxene occurs most efficiently around 3.5 eV. These optical properties of annealed siloxene are consistent with the indirect nature of the  $\text{Si}_6$  ring band gap in Fig. 3. Luminescence and the onset of absorption are expected at the lowest (indirect) gap. On the other hand, efficient luminescence excitation should occur at energies between 3.5 and 4 eV, where direct optical transitions within individual  $\text{Si}_6$  rings are possible.

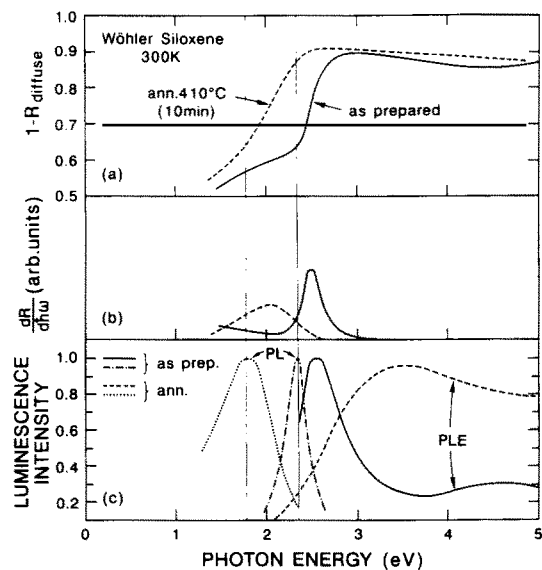


Fig. 6. Comparison of the room temperature optical properties of as-prepared and annealed (410°C, 10 min.) siloxene: (a) optical absorption obtained from the diffuse reflectivity; (b) first derivative of the reflectivity with respect to the photon energy, emphasizing the sharpness and the position of the absorption edge; (c) photoluminescence (PL) and luminescence excitation spectra (PLE).

#### 4. Luminescence in siloxene and porous silicon

We now turn to the most interesting optical property of siloxene, namely its strong visible luminescence. In the following section, we shall describe various characteristic features of this luminescence and compare them to corresponding properties of porous silicon. Our aim is to provide a brief overview over radiative recombination in siloxene and siloxene derivatives, but also to show to what extent features of the luminescence in siloxene and porous Si agree, in order to give additional evidence for our earlier claim that certain siloxene derivatives are the structural origin of visible room temperature luminescence in porous Si.

First, we present in Fig. 7 a comparison between the luminescence spectra of as-prepared and annealed siloxene as well as three different porous Si samples. All spectra were recorded at 300 K under identical conditions, and only the intensity scale was normalized. This normalization is necessary

because the emission intensity of typical porous Si samples may vary by more than one order of magnitude, and also because thermal annealing of siloxene creates a large density of Si-related coordination defects (dangling bonds), which act as non-radiative recombination centers and strongly quench the luminescence at 300 K. Estimated external quantum efficiencies for the samples shown in Fig. 7 are between 1 and 20%. We note that annealed siloxene radiates in the same spectral range as porous Si, namely 600–850 nm, with long tails extending up to 500 nm and deep into the infrared region. The large width of the luminescence band in annealed siloxene compared to porous Si is most likely due to structural inhomogeneities (different degrees of oxidation of Si<sub>6</sub> rings). As-prepared siloxene, on the other hand, has its maximum emission in the vicinity of 520 nm, with very little intensity in the red spectral region characteristic for porous Si. Thus, we conclude that a connection between the origin of luminescence in porous silicon and in siloxene has to be in the complex amorphous-like structure of annealed

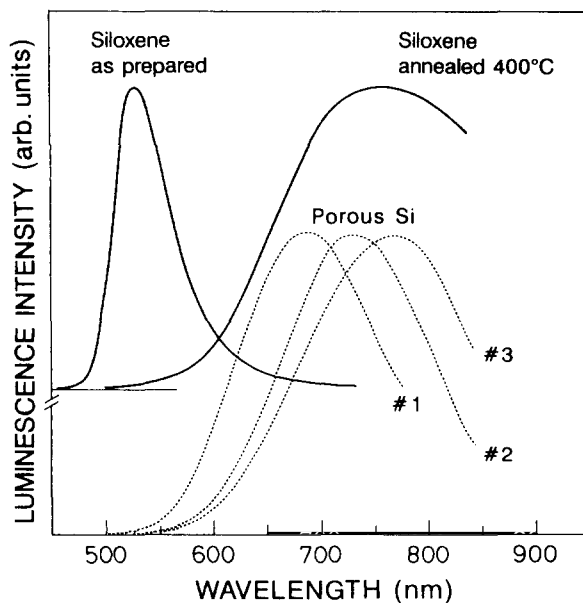


Fig. 7. Photoluminescence spectra of as-prepared siloxene, siloxene annealed at 400°C and three different porous silicon samples.

siloxene rather than in the ordered two-dimensional Si planes present in as-prepared siloxene.

As shown in Fig. 8, the luminescence intensity in as-prepared and in annealed siloxene is essentially proportional to the excitation intensity over six orders of magnitude. This observation is valid both at 77 and at 300 K, indicating that radiative recombination occurs mainly from geminate pairs and is little affected by bimolecular or Auger recombination processes. The same observation also holds for porous Si [16]. In addition, one can see from Fig. 8 that the luminescence intensity increases by about one order of magnitude upon cooling from

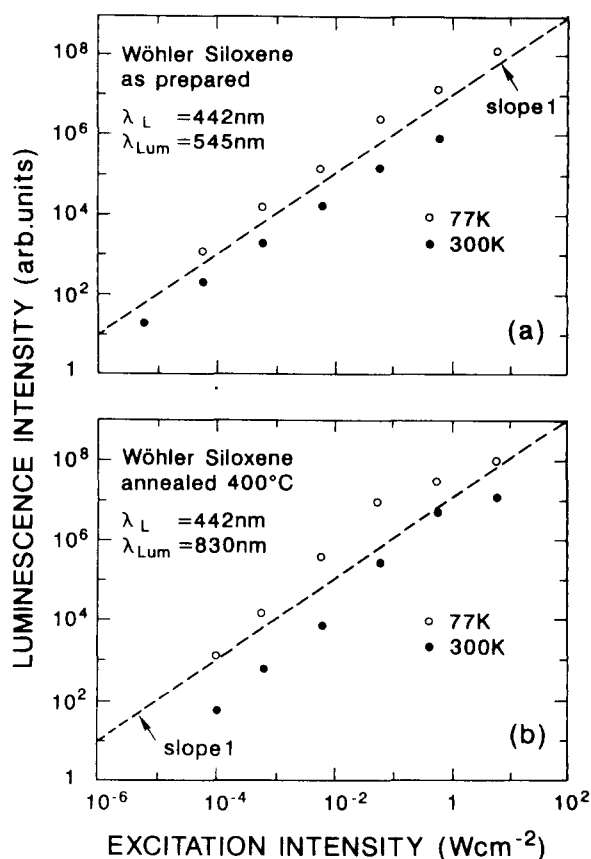


Fig. 8. Dependence of the luminescence intensity on excitation intensity in as-prepared siloxene (upper part) and annealed siloxene (lower part).  $\lambda_L$  and  $\lambda_{lum}$  denote the excitation wavelength and the luminescence monitor wavelength, respectively. Solid and open symbols refer to luminescence at 77 and at 300 K, respectively.

300 K to 77 K. As discussed in detail by Rosenbauer et al. in the present volume [17], the temperature dependence of the luminescence both in porous Si and in siloxene is well described by the relation

$$\frac{I_0}{I(T)} = 1 + \exp(T/T_0) \quad (1)$$

with a characteristic temperature  $T_0$  between 50 and 100 K.

Time-resolved decay curves of the luminescence intensity following excitation with a short laser pulse are depicted in Fig. 9. A characteristic feature observed in porous Si as well as in siloxene is a non-

exponential decay which becomes faster with shorter wavelengths monitored [18,19]. In porous Si, the characteristic decay times for the majority of the radiative states is about 1 ms at 4 K and 0.1 ms at 300 K. According to Fig. 9, quite similar lifetimes are observed in annealed siloxene (1 ms and 10  $\mu$ s, respectively). The shorter luminescence decay time at room temperature in annealed siloxene is most likely due to the faster non-radiative quenching of the luminescence caused by the very high density of defect states ( $\approx 10^{18} \text{ cm}^{-3}$ ). Even shorter lifetimes (in the ns regime) have been observed in as-prepared siloxene [6,20]. More details concerning time-resolved luminescence measurements in porous Si and siloxene are presented by Finkbeiner et al. in this volume [19].

In Fig. 6, we have already shown photoluminescence excitation (PLE) spectra of siloxene in the as-prepared and the annealed state. In Fig. 10, we

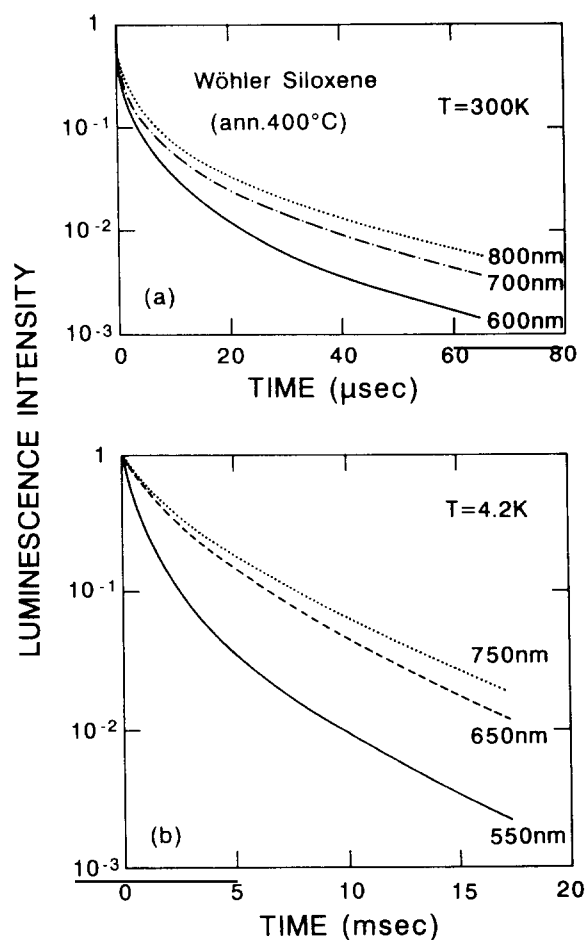


Fig. 9. Transient decays of the luminescence in annealed Wöhler siloxene at 300 K (a) and at 4.2 K (b). Different curves were obtained by monitoring the indicated luminescence wavelengths.

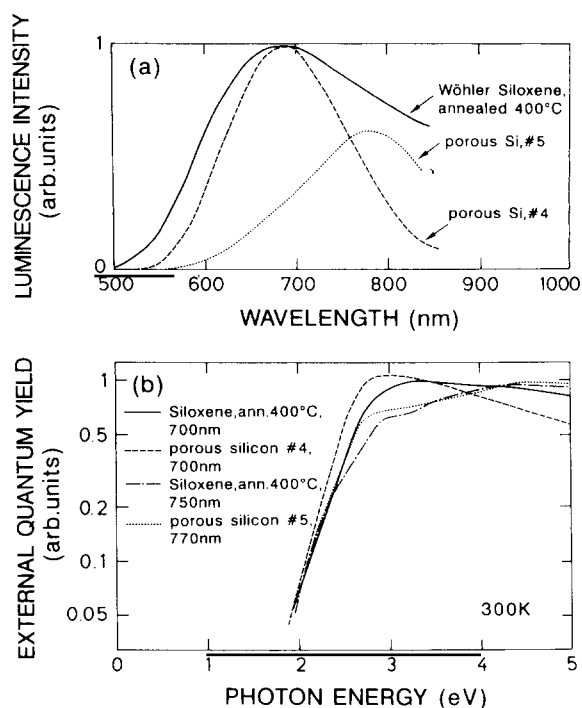


Fig. 10. Photoluminescence (a) and luminescence excitation spectra (b) of annealed siloxene and two porous Si samples. Different curves in (b) correspond to different luminescence monitor energies as indicated in the figure. Note the semi-logarithmic plot in (b).

present more details concerning PLE in annealed siloxene and in porous Si. Fig. 10(a) depicts the room temperature luminescence spectra of the samples whose PLE spectra are compared in Fig. 10(b) [21]. Again we see a very close agreement between spectra recorded in porous silicon and in annealed siloxene at the same luminescence wavelength. In addition, the semilogarithmic plot in Fig. 10(b) indicates that the low-energy end of the PLE spectra in all samples decays with an exponential tail, the slope parameter  $\ln\eta/dh\nu$  of which is typically 200 meV ( $\eta$  is PLE quantum yield,  $h\nu$  is photon energy). This exponential tail occurs in the same energy range (2–2.5 eV) as the optical gap of annealed siloxene (cf. Fig. 6) and is indicative for excitation of luminescence by absorption in a substoichiometric Si–O alloy.

The discussion of the luminescence properties of annealed siloxene given so far indeed provides a lot of indirect evidence for our suggestion that porous Si and annealed siloxene exhibit a common structural origin of visible luminescence, e.g. Si<sub>6</sub> rings. A proof of this hypothesis requires clear microscopic information directly related to the electronic wave functions from which radiative recombination occurs. The only method capable of providing such information is ODMR, in which changes of the luminescence intensity produced by resonant spin–flip transitions are monitored. A detailed description of this technique is certainly beyond the scope of the present review, and the interested reader is referred to the relevant literature. Also, we will only describe the most basic results of our recent ODMR investigation in porous Si and siloxene, with many details left for forthcoming publications [22].

We begin by showing in Fig. 11 ODMR spectra obtained from different porous Si samples and from annealed siloxene under identical experimental conditions. The characteristic features of these spectra are

- A broad enhancing signal (i.e. a resonant increase of the luminescence intensity) at magnetic fields around 3300 G due to triplet excitons. Proof for the existence of triplet excitons comes from the sharper resonance line at exactly half the magnetic field (1650 G) due to the (forbidden) simultaneous spin–flip transition ( $\Delta m_s = 2$ ) of

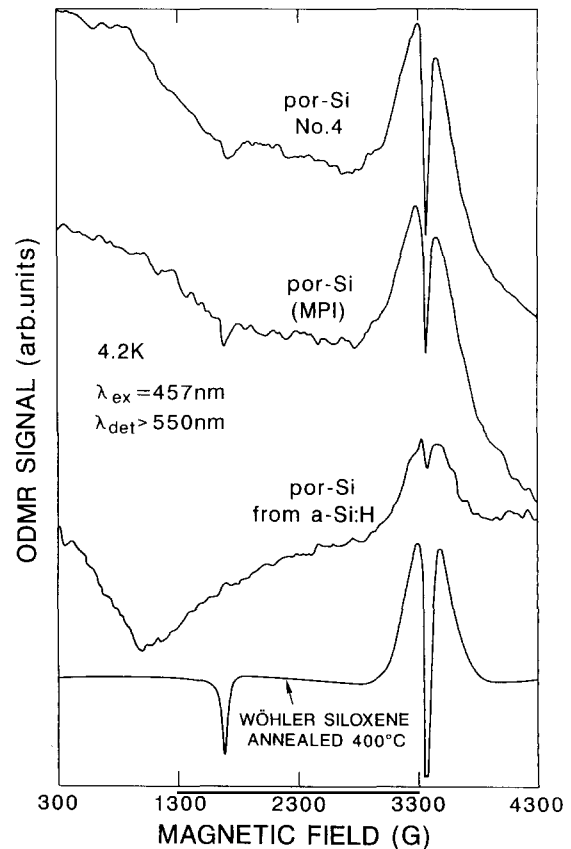


Fig. 11. Optically detected magnetic resonance (ODMR) spectra of different porous silicon samples and of annealed siloxene at 4.2 K.  $\lambda_{\text{ex}}$  and  $\lambda_{\text{det}}$  are the laser excitation wavelength and the detector cutoff wavelength, respectively.

both electronic spins (electron and hole) forming the radiant triplet exciton. The integrated enhancement of the luminescence due to microwave-induced triplet exciton spin–flips is typically of the order of 10% at 4.2 K. This large effect ensures that our ODMR measurements in fact are sensitive to the majority of all radiative transitions in porous Si and siloxene, rather than representing a small subset of all possible transitions. The  $g$ -value of the triplet exciton calculated as half the  $g$ -value of the forbidden  $\Delta m = 2$  transition is  $g = 2.01$  both in porous Si and in annealed siloxene. Indirect evidence for triplet excitons in porous Si has previously been deduced from the temperature dependence of the luminescence lifetime [24].

- A sharp quenching signal (decrease of the luminescence intensity) at about 3350 G ( $g = 2.005$ ) due to resonance-induced non-radiative recombination at structural defects (dangling bonds). Note that this signal is relatively stronger in annealed siloxene because of the larger density of such defects. More details concerning this defect-related signal have been published elsewhere [23].
- Porous Si samples prepared and measured on crystalline Si substrates always exhibit a broad background signal with some structure around 1000 G due to microwave-induced cyclotron resonance in the substrate. This resonance influences the luminescence intensity only indirectly via thermal heating of the substrate, and can appear as an enhancing or as a quenching signal depending on whether the temperature coefficient  $dI/dT$  of the porous layer is positive or negative. This background is obviously absent in siloxene.

For an understanding of the origin of luminescence in porous Si, the most interesting feature of the ODMR spectra in Fig. 11 is the broad enhancing resonance of the triplet excitons. The width of this line, which is directly related to the effective radius of the triplet exciton (either via dipolar or via exchange interaction), is plotted in Fig. 12 as a function of the cutoff energy of the optical filter (low pass) used for the ODMR experiments. We can see from Fig. 12 that in all porous Si samples this width is about 500 G, irrespective of the monitored photon energy or of the method employed for the preparation of the porous Si layer. Also, a similar width is seen in annealed siloxene, especially after aging in air. In contrast, the ODMR line width and the spectral shape are quite different in as-prepared siloxene or, for example, in amorphous Si.

An important consequence of the ODMR results in Fig. 12 is that the large luminescence line width in porous Si cannot be due to a size distribution of Si crystallites or wires, as postulated by the conventional quantum confinement model. The width of the triplet exciton resonance in ODMR should vary with the excitonic radius  $r$  either as  $r^{-3}$  or as  $\exp\{-2ar\}$ , depending on whether dipolar spin-spin interaction or exchange interaction dominates. Thus, purely dipolar interaction between the

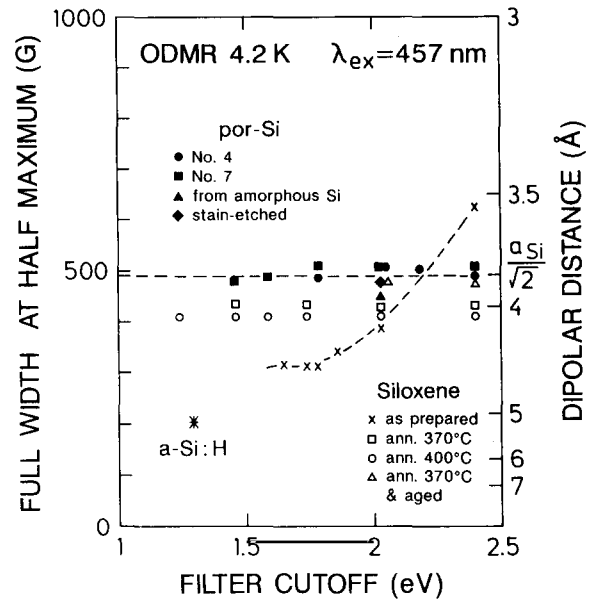


Fig. 12. Compilation of triplet exciton ODMR linewidths in porous Si samples (closed symbols), as-prepared siloxene (crosses), annealed siloxene (open symbols) and amorphous hydrogenated Si (a-Si:H, star) at 4.2 K as a function of the cutoff energy of the luminescence detector.

two spins forming the triplet state in an isotropic sample gives rise to a Pake doublet with a splitting

$$\Delta H \approx g\mu_B/r^3, \quad (2)$$

where  $\mu_B$  is the Bohr magneton and  $r$  is the spin-spin distance. The broad enhancing line in porous Si as well as in annealed siloxene can be well fitted by such a Pake doublet convoluted with a Gaussian broadening function of about 70 G width. Irrespective of the detailed line shape analysis, one can state qualitatively that the variation in the excitonic radius  $r$  necessary to produce the observed variation in the luminescence energy in the context of the quantum confinement model should have a very large effect on the ODMR line width, which is clearly not observed. Second, from the comparison with as-prepared siloxene and with amorphous Si, we can also exclude the possibility that the luminescence in porous Si originates from a disordered a-Si:H phase or from the extended two-dimensional Si planes characteristic for as-prepared siloxene. Instead, the ODMR data are

consistent with our model that isolated Si<sub>6</sub> rings present in both porous Si and annealed siloxene are responsible for the observed luminescence: the diameter of such rings is about 4 Å, exactly what is required for a triplet exciton with a dipolar interaction corresponding to the observed ODMR line width of 400–500 G, and the variation of the ring luminescence energy by ligand effects described further above can account for the observation of an excitonic radius almost independent of luminescence energy.

### 5. Summary and conclusions

We have presented a brief review over the optical properties of siloxene, with special emphasis on annealed siloxene and its relevance for the luminescence observed in porous Si. For a detailed understanding, many structural and electronic properties of siloxene still require intensive investigations. Nevertheless, we begin to appreciate in particular the unique luminescence properties of siloxene and their connection with two basic structural components, namely two-dimensional Si planes and isolated Si<sub>6</sub> rings. We have also discussed many properties of annealed siloxene and porous Si which indicate the existence of a common structural origin underlying the strong visible luminescence observed for both materials. Especially the microscopic information provided by our recent ODMR measurements casts strong doubt on the established quantum confinement picture of luminescence in porous Si, but agrees well with isolated Si<sub>6</sub> rings as the main radiative center.

### References

- [1] F. Wöhler, *Liebigs Ann. Chem.* 127 (1863) 257.  
 [2] H. Kautsky and G. Herzberg, *Z. Anorg. Allg. Chem.* 139 (1924) 135.  
 [3] E. Hengge and K. Pretzer, *Chem. Ber.* 96 (1963) 470.  
 [4] A. Weiss, G. Beil and H. Meyer, *Z. Naturforsch* 35 b (1980) 25.  
 [5] H. Ubara, T. Imura, A. Hiraki, I. Hirabayashi and K. Morigaki, *J. Non-Cryst. Solids* 59/60 (1983) 641.  
 [6] I. Hirabayashi, K. Morigaki and S. Yamanaka, *J. Non-Cryst. Solids* 59/60 (1983) 645.  
 [7] M.S. Brandt, H.D. Fuchs, M. Stutzmann, J. Weber and M. Cardona, *Solid State Commun.* 81 (1992) 307.  
 [8] M. Stutzmann, J. Weber, M.S. Brandt, H.D. Fuchs, M. Rosenbauer, P. Deak, A. Höpner and A. Breitschwerdt, *Adv. Solid State Phys.* 32 (1992) 179.  
 [9] S.L. Friedman, M.A. Marcus, D.L. Adler, Y.-H. Xie, T.D. Harris and P.H. Citrin, *Appl. Phys. Lett.* 62 (1993) 1934.  
 [10] T.K. Sham et al., *Nature* 363 (1993) 331.  
 [11] R.F. Pinizzotto, H. Yang, J.M. Perez and J.L. Coffer, submitted to *Appl. Phys. Lett.*  
 [12] M.S. Brandt, A. Breitschwerdt, H.D. Fuchs, A. Höpner, M. Rosenbauer, M. Stutzmann and J. Weber, *Appl. Phys. A* 54 (1992) 567.  
 [13] H.D. Fuchs, M. Stutzmann, M.S. Brandt, M. Rosenbauer, J. Weber, A. Breitschwerdt, P. Deak and M. Cardona, *Phys. Rev. B*, in press.  
 [14] P. Deak, M. Rosenbauer, M. Stutzmann, J. Weber and M.S. Brandt, *Phys. Rev. Lett.* 69 (1992) 2531.  
 [15] C.G. Van de Walle and J.E. Northrup, *Phys. Rev. Lett.* 70 (1993) 1116.  
 [16] H.D. Fuchs, M. Stutzmann, M.S. Brandt, M. Rosenbauer, J. Weber and M. Cardona, *Phys. Scr. T* 45 (1992) 309.  
 [17] M. Rosenbauer, M. Stutzmann, H.D. Fuchs, S. Finkbeiner and J. Weber, *J. Lumin.* 57 (1993) 153.  
 [18] J.C. Vial, A. Bsiesy, F. Gaspard, R. Herino, M. Ligeon, F. Muller, R. Romestain and R.M. MacFarlane, *Phys. Rev. B* 45 (1992) 14171.  
 [19] S. Finkbeiner, J. Weber, M. Rosenbauer and M. Stutzmann, *J. Lumin.*, 57 (1993) 231.  
 [20] M. Stutzmann, M.S. Brandt, H.D. Fuchs, M. Rosenbauer, M.K. Kelly, P. Deak, J. Weber and S. Finkbeiner, *Proc. NATO Adv. Research Workshop, Yountville, CA (Kluwer, Dordrecht, 1993)* in print.  
 [21] M. Stutzmann, M.S. Brandt, M. Rosenbauer, J. Weber and H.D. Fuchs, *Phys. Rev. B* 47 (1993) 4806.  
 [22] M.S. Brandt and M. Stutzmann, in preparation.  
 [23] M.S. Brandt and M. Stutzmann, *Appl. Phys. Lett.* 61 (1992) 2569.  
 [24] P.D.J. Calcott, K.J. Nash, L.T. Canham, M.J. Kane and D. Brumhead, *J. Phys.: Condens. Matter* 5 (1993) L91.